Impact of Fe doping on the electronic structure of $SrTiO_3$ thin films determined by resonant photoemission

J. Kubacki, D. Kajewski, J. Goraus, K. Szot, A. Koehl, Ch. Lenser, R. Dittmann, and J. Szade

Citation: The Journal of Chemical Physics **148**, 154702 (2018); doi: 10.1063/1.5007928
View online: https://doi.org/10.1063/1.5007928
View Table of Contents: http://aip.scitation.org/toc/jcp/148/15
Published by the American Institute of Physics

Impact of Fe doping on the electronic structure of $SrTiO_3$ thin films determined by resonant photoemission

J. Kubacki,[1,2,a)] D. Kajewski,[1] J. Goraus,[1,2] K. Szot,[1,3] A. Koehl,[3] Ch. Lenser,[3] R. Dittmann,[3] and J. Szade[1,2]

[1]*A. Chełkowski Institute of Physics, University of Silesia, Katowice 40-007, Poland*
[2]*Silesian Center for Education and Interdisciplinary Research, Chorzów, Poland*
[3]*Peter Grünberg Institut, Forschungszentrum Jülich, 52425 Jülich, Germany*

(Received 4 October 2017; accepted 16 March 2018; published online 16 April 2018)

Epitaxial thin films of Fe doped $SrTiO_3$ have been studied by the use of resonant photoemission. This technique allowed us to identify contributions of the Fe and Ti originating electronic states to the valence band. Two valence states of iron Fe^{2+} and Fe^{3+}, detected on the base of x-ray absorption studies spectra, appeared to form quite different contributions to the valence band of $SrTiO_3$. The electronic states within the in-gap region can be attributed to Fe and Ti ions. The Fe^{2+} originating states which can be connected to the presence of oxygen vacancies form a broad band reaching binding energies of about 0.5 eV below the conduction band, while Fe^{3+} states form in the gap a sharp feature localized just above the top of the valence band. These structures were also confirmed by calculations performed with the use of the FP-LAPW/APW+lo method including Coulomb correlations within the d shell. It has been shown that Fe doping induced Ti originating states in the energy gap which can be related to the hybridization of Ti and Fe 3d orbitals. *Published by AIP Publishing.* https://doi.org/10.1063/1.5007928

I. INTRODUCTION

The $SrTiO_3$ (STO) can be regarded as a model oxide with the perovskite structure. Its bandgap of 3.2 eV, high dielectric constant, and paraelectric state at room temperature make STO an interesting material for applications in emerging oxide electronics. Electrical conductivity of STO can be tuned by chemical doping, oxygen deficit, or formation of interfaces with other perovskites as in the case of the $LaAlO_3$/STO systems.[1] Moreover, local insulator-metal transitions were observed at the nanoscale level, which were attributed to a strong coupling of the structural inhomogeneity and the modified electronic structure.[2] Doping and the presence of defects or interfaces can lead to modifications of the energy gap region via the formation of new electronic states and transformation of the electronic wavefunctions from the localized to itinerant character. Therefore, knowledge on the electronic states responsible for such transformations is crucial to understand the electrical properties of a material which is insulating when undoped and structurally unchanged.

Slightly Fe doped STO is a model representative for the acceptor doped large bandgap electroceramics.[3,4] The mixed valence (Fe^{3+}/Fe^{4+}) character of the dopant creates a charge imbalance with respect to the lattice which is compensated by oxygen vacancies (V_O) in a large oxygen partial pressure regime.[5,6] Full substitution of Ti by Fe leads to a metallic perovskite compound—$SrFeO_3$ which has a different structure than STO and is a helical antiferromagnet with T_N = 134 K.[7] In the recent paper, da Silva *et al.* have shown that synthesis of the $Sr(Ti, Fe)O_3$ powders with nanometer-sized particles by the polymeric precursor method leads to formation of the cubic perovskite structure in the whole substitution range.[8,9] They showed that $Sr(Ti, Fe)O_3$ is a mixed (ionic and electronic) conductor and that the electronic contribution becomes dominant with increasing Fe content. Other theoretical approaches to the Fe doping effects have shown the formation of the electronic in-gap states. Their degree of localization and bandwidth depend on the doping level, the assumed Fe valence, and the method employed for the calculations.[10–12]

For the majority of applications, the use of thin films is inevitable. Due to the strongly kinetically limited growth conditions in many widely used thin film deposition methods, e.g., pulsed laser deposition (PLD) and sputtering, the formation of defects and the incorporation of dopants into the crystal lattice considerably differ from single crystals and bulk ceramics. The Fe doped STO films exhibit, even when they are grown at high oxygen pressure, no significant Fe^{4+} contribution.[13] Analysis of the Fe 2p photoemission multiplet in single crystalline STO thin films showed that for doping levels of Fe up to 2%, its valence state is rather a combination of 2+ and 3+ with a divalent contribution situated mostly on the surface.[14] The x-ray absorption spectroscopy (XAS) confirmed the mixed valence state of iron and have shown that it is independent of the doping concentration and that annealing increases the relative Fe^{2+} signal ratio.[14] Our XPS results obtained for Fe doped STO films indicated a clear relation between doping and the increased density of states in the energy gap.[15] The effect of doping was discussed in terms of coherent and incoherent electronic states mainly for electron doping as it was done for Nb replacing Ti in STO.[16] It was also shown that thermal reduction of undoped STO leads to the appearance of metallic-like bands crossing the Fermi level.[17,18] However, no detailed

a)Author to whom correspondence should be addressed: jerzy.kubacki@us.edu.pl. Tel.: +48 32 3497563. Fax: +48 32 2588431.

studies of the in-gap electronic structure for acceptor-like dopants such as Fe have been reported so far.

In this paper, we aim to clarify the role of Fe in the modification of the electronic structure of STO thin films. By using resonant photoemission, we were able to determine the partial densities of states for Fe and Ti. We also show that taking into account XAS and photoemission data, we are able to clearly distinguish between the contribution of divalent and trivalent iron ions to the electronic states in the valence band. We determined also electronic states in the energy gap which originated from the Ti states and investigated how they depend on iron doping.

The experimental data have been compared with calculations performed using the FP-LAPW/APW+lo method for the 3.7% Fe doping level and by including the Coulomb correlation within the 3d shell.

II. EXPERIMENTAL SECTION

Thin films of $SrTiO_3$ (STO) undoped and doped with Fe were grown by pulsed laser deposition (PLD) using a KrF excimer laser and ceramic targets with nominal composition $SrTiO_3$, $SrTi_{0.99}Fe_{0.01}O_3$, $SrTi_{0.98}Fe_{0.02}O_3$, and $SrTi_{0.95}Fe_{0.05}O_3$, respectively. The films were about 20 nm thick. The substrates were commercially available (001) oriented conducting Nb:STO single crystals in order to prevent charging during spectroscopic investigations. The deposition process was performed with an oxygen partial pressure of 0.25 mbar at a repetition rate of 5 Hz and a laser energy density of 0.8 J/cm^2. The substrate was kept at a temperature of 700 °C. X-ray diffraction and low energy electron diffraction (LEED) examination confirmed the epitaxial growth of the deposited films. However, formation of very low amount of other phases cannot be ruled out due to the limited sensitivity of x-ray diffraction.

Photoelectron spectroscopy measurements and the X-ray absorption spectroscopy (XAS) were performed at the I311 beamline in a Max-lab synchrotron. The X-ray beam size was of the order of $100 \times 500\ \mu m^2$. The XAS spectra were obtained by the Auger electron yield (AEY) method based on intensity changes of a selected Auger electron peak.

The films were annealed prior to the measurements in UHV conditions at temperatures of 150 °C, 300 °C, or 630 °C. The vacuum level was of the order of 10^{-8}–10^{-9} mbar during the annealing. Heating removed most of carbon contaminations. Some remaining carbon and minor contribution of oxygen species not attributed to the perovskite structure were detected for most samples. The effect of these contaminations was estimated and found to be irrelevant for the studies of the Fe electronic state.

Ab initio calculations of STO were performed by the FP-LAPW/APW+lo method as implemented in Wien2K14 code[19] using local-density approximation (LDA) potential in the form proposed by Perdew and Wang[20] with Ceperley-Adler parametrization.[21] The Coulomb correlation within the transition metal 3d shell was studied using the local spin density approximation LSDA+U method proposed by Anisimov *et al.*[22] for U = 6 eV. The calculations for the STO system doped with iron were performed for a 3 × 3 × 3 STO unit cell, where the central atom (Ti) of the middle unit cell was substituted by an iron atom. Such a structural model corresponds to 3.7% Fe doping and preserves the high cubic symmetry of the original unit cell. Vacancies at the oxygen sites were simulated within virtual crystal approximation, where an atom with an effective atomic number Z = 7.95 was placed at all oxygen positions, and the charge neutrality of the unit cell was preserved. The **k**-space integrations were done using 20 **k**-points in the irreducible wedge of the Brillouin zone for the supercell and 455 k-points for the pristine compound. All calculations were converged better than 0.01 meV with respect to total energy and better than 0.001 *e* with respect to charge. The plane wave cut-off factor of $R_{MT}\ K_{max} = 7.0$ and the convergence with respect to k-grid and $R_{MT}K_{max}$ were carefully checked.

III. RESULTS AND DISCUSSION

The resonant photoelectron spectroscopy (RESPE) is a technique which requires measurements of the photoelectron spectra for photon energies within the region of a selected absorption edge. Acquiring of the XAS spectrum is thus a first step for the RESPE studies.

Analysis of the XAS spectra obtained for the undoped STO film and the films with an Fe content up to 5% allowed us to distinguish between the Fe^{2+} and Fe^{3+} contribution to the observed spectra and to the state that the XAS Fe L edge spectra have the same structure for all films. All spectra have two well resolved maxima within the L_3 edge and at least three components of the L_2 edge. Figure 1 presents the example of the Fe $L_{2,3}$-edge XAS spectrum for the 2% Fe doped $SrTiO_3$ film measured in Auger electron yield mode after annealing the sample at 300 °C for 30 min in a ultra-high vacuum. The extended analysis of the XAS spectra obtained for the analogous thin films of STO was done in the paper by Koehl *et al.*[15] The spectra of the L_3 edge have two main peaks at 708.3 eV and 710 eV plus a low energy shoulder for all concentrations of Fe and all used methods of sample preparation. However, the ratio of two main components within the XAS spectra showed significant differences between the samples prepared in various ways and for two used methods of acquisition AEY

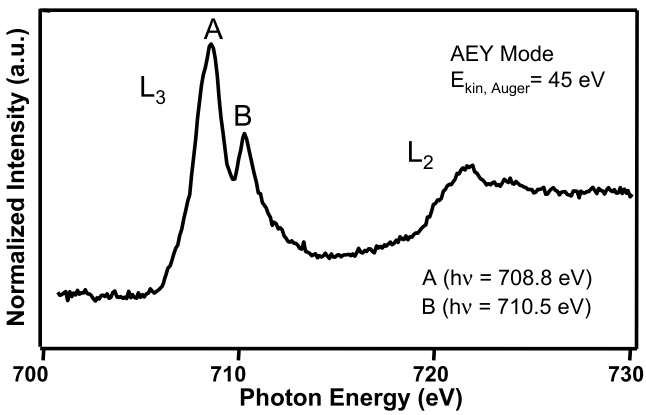

FIG. 1. Fe L edge x-ray absorption spectrum obtained in the Auger electron yield mode for the STO film doped with 2% Fe. Peaks described as A and B can be attributed to mostly divalent and trivalent Fe ions according to the reasoning presented in the text.

and TEY (total electron yield) which exhibit different surface sensitivity.

The observed maximum at about 708.8 eV (marked as "A") comes mostly from the Fe^{2+} contribution to the Fe L_3 absorption edge spectrum. The second observed maximum at 710.5 eV (marked as "B") can be attributed mostly to the Fe^{3+} contribution.[15] However, one has to remember that the calculated structure of the XAS spectra shows some contributions from both valence states within the peaks A and B.

Calculations based on atomic multiplet theory plus crystal field and charge transfer (the CTM4XAS program by Stavitski and de Groot) compared to the experimental spectral showed that the relative Fe^{2+} contribution varies from 23% (48%) to 43% (69%) depending on the annealing temperature and mode of acquisition—TEY (AEY), respectively. The interpretation of the Fe L edge XAS spectra is in agreement with the analysis performed for other Fe containing oxides.[23,24] A clear difference in the resonance behavior of the valence band, discussed below, for the photon energies being very close to each other can confirm the different electronic configurations responsible for the appearance of peaks A and B.

The photoemission map of the valence band for the photon energy range of the Fe 2p-3d resonance is presented in Fig. 2. The map shows the photoemission intensity as a function of binding energy and photon energy. The scale of intensity was tuned to highlight subtle effects in the in-gap binding energy range. The main contribution is placed in the region of the valence band formed by the O, Sr, and Ti orbitals, i.e., between 3 and 7 eV. This region was investigated many times for STO and the mentioned assignment of the electronic states is in agreement with the resonant photoemission studies of STO and calculations.[9] It is also noteworthy that some enhancement of photoemission is observed in the energy range over 8 eV where the electronic states are most likely related to defects.[25] In the photon energy range of the Fe L_3 absorption edge, one can notice a clear resonant enhancement of the in-gap electronic states.

Surprisingly, there are almost no observable changes of the photoemission for the photon energy range of the L_2 edge. Such a situation can be expected only when a high spin state of the Fe 3d level is realized and spin forbidden transitions are damping the resonance effect. Due to the spin exchange interaction and spin-orbit splitting, the L_2 ($2p_{1/2}$) sublevel is spin polarized opposite to the majority spin of the 3d level. During the 2p-3d absorption process, only the minority spin levels are virtually occupied. The resonant photoemission is then blocked from the occupied majority spin 3d sub-bands. In the high spin Fe $3d^5$ state, it concerns both crystal field split sublevels t_{2g} and e_{2g}. Having the XAS spectra for all investigated samples, we could perform resonant photoemission spectroscopy of the valence band with the use of three different photon energies, to obtain partial (projected) density of states (PDOS) which, according to the discussion presented in our previous paper, corresponds mostly to Fe^{2+} and Fe^{3+}.

Two chosen photon energies were equal to the energies of the peaks A and B, and the third one was chosen for the off-resonance energy which was about 700 eV. In order to obtain PDOS of iron, we subtracted spectra obtained for the on- and off-resonance energies after normalizing the spectra with the use of beam intensity. Figure 3 shows three spectra obtained at energies of 700, 708.8, and 710.5 eV.

Iron dependent DOS's for Fe^{2+} and Fe^{3+}, calculated as described above, are presented in Fig. 4. Measurements were performed for three concentrations of iron in the films: 1, 2, and 5 at. % and for two different ways of thermal treatment.

Several important features can be noticed—the structure of the Fe PDOS is quite different for two photon energies on resonance. It seems thus reasonable to attribute the obtained densities of states to Fe^{2+} and Fe^{3+}. We will refer further in the text to the 3+ and 2+ iron valence states having in mind that this assignment is valid on the base of the XAS analysis and data from the literature.[15]

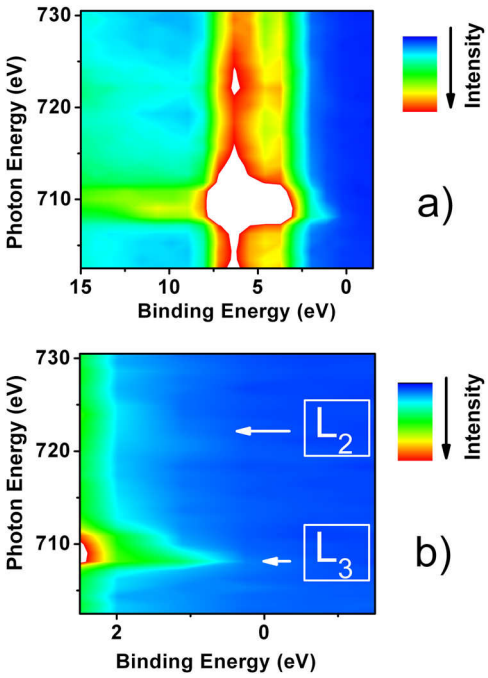

FIG. 2. (a) Photoemission intensity maps in the valence band region obtained for the 2% Fe doped STO film for photon energies within the Fe 2p-3d resonance. Panel (b) shows the zoomed region of the energy gap.

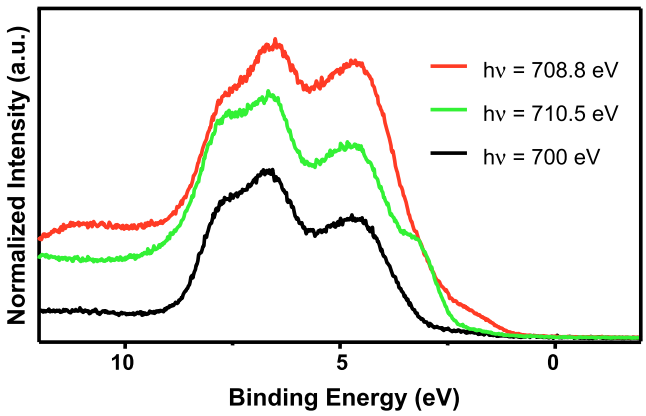

FIG. 3. Selected valence band photoemission spectra for the 2% Fe doped STO film, obtained for photon energies on- and off-resonance. Photon energies of 708.8 eV and 710.5 eV correspond to the positions of the peaks in the XAS spectrum. 700 eV is the off-resonance photon energy.

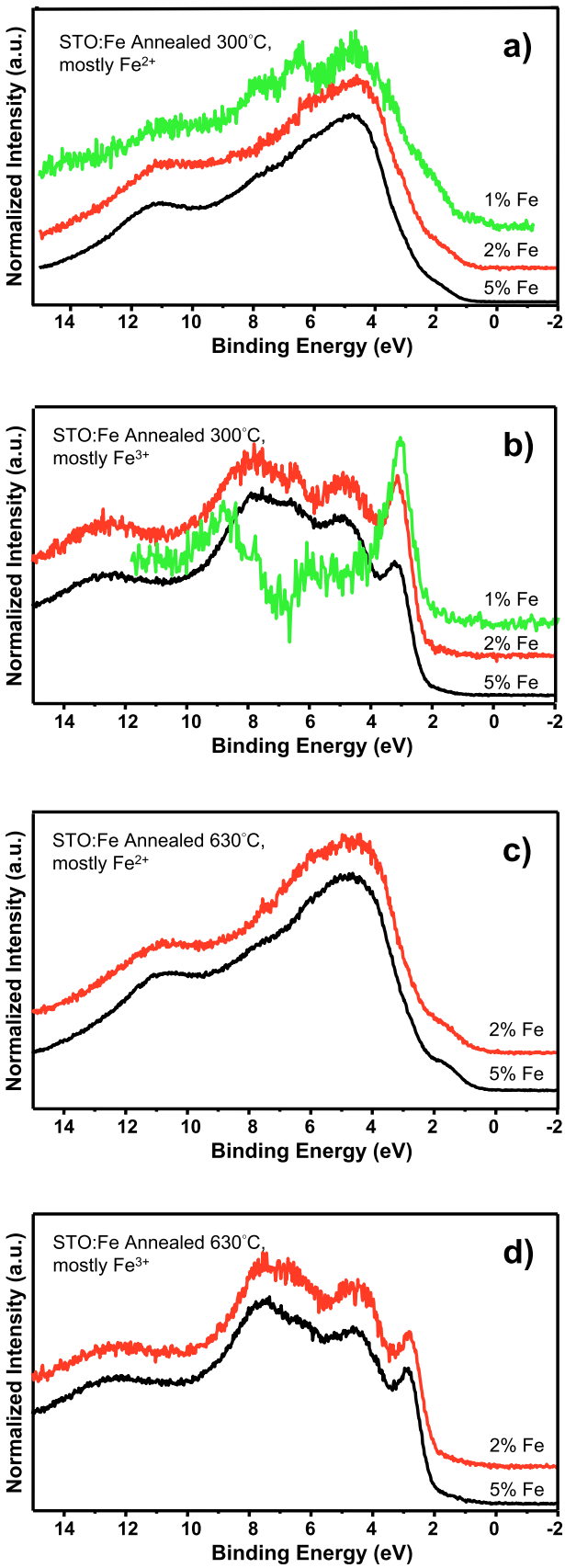

FIG. 4. Fe partial densities of states (PDOS's) obtained for the resonance I corresponding to a photon energy of 708.8 eV and peak A in the XAS spectra (a) and (c) and for photon energy of resonance II—peak B (710.5 eV)—panels (b) and (d). Panels (a) and (b) correspond to films annealed at 300 °C prior to the measurements, while panels (c) and (d) were obtained for annealing at 630°.

Figure 5 shows the resonant behavior of the in-gap states presented in the CIS (constant initial state) mode for photon energy range of the Fe L absorption edge. The enhancement of the Fe originating states is well visible for binding energies starting from about 0.5 eV. No states at the Fermi level are observed which is in agreement with the classical description of acceptor states above 1 eV from the valence band for low Fe doping.[26]

The structure is different for the main part of the DOS, i.e., for binding energies between 3 and 8 eV and within the bandgap. For the Fe^{2+} DOS, the contribution to in-gap states is much more pronounced and extends to binding energies of about 0.5 eV—very close to the Fermi level. For the Fe^{3+}, the electronic states form a more complicated structure. The most interesting feature is a distinct peak situated at 2.5 eV, so just above the top of the valence band. Its evolution with the Fe concentration is also interesting. It is the most pronounced for the lowest Fe concentration. It allows us to relate the electronic state to acceptor like states coming from the isolated doping ions. The position of the peak agrees roughly with data for the ionization energy of Fe optical centers in STO. Increasing doping level leads probably to more non-homogeneous Fe distribution and finally to formation of less localized electronic states. We found no effect described in the studies of da Silva *et al.* and Rotschild *et al.*,[9,27] where the gradual decrease of the energy gap was detected with increasing Fe content at least in the concentration region studied in our films.

The results of our calculations are shown in Fig. 6. As is common for the LDA method, the width of the energy gap is slightly smaller than in the experiment. Adding the correlation within the 3d levels removes the states originating from Fe in the middle of the energy gap. The value of correlation energy of 6 eV was chosen arbitrary, based on the obtained experimental results, in order to check this effect. The most prominent contribution from Fe to the DOS is situated just above the top of the valence band. A slight effect is visible also at the bottom of the conduction band where Fe substitution leads to lowering of the band limit. The method we used does not allow us to obtain the Mulliken net charge for the Fe atom placed in the center of the octahedron. A strong contribution visible at about 2.5 eV in PDOS derived from the experiment is reflected in

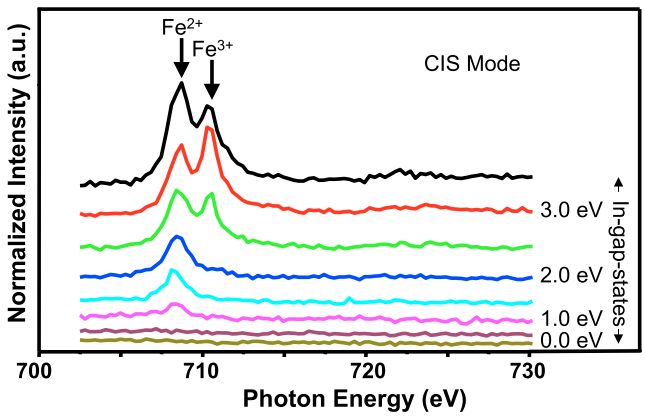

FIG. 5. Photoelectron intensity obtained for the 2% Fe doped STO film in the CIS mode presenting the photon energy dependence of the in-gap states.

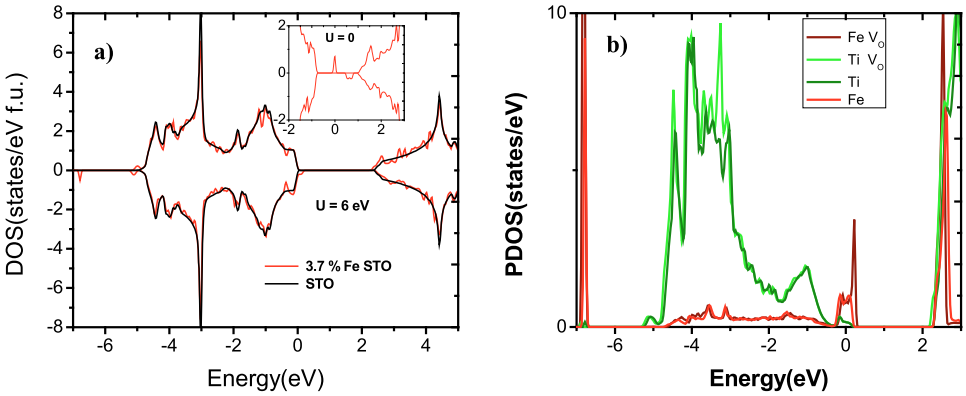

FIG. 6. Density of states obtained from FP-LAPW calculations, (a) STO and 3.7% Fe STO, the inset shows the region of the bandgap calculated without correlation energy and (b) density of states projected on Ti and Fe and the effect of oxygen vacancies (V_o) simulated by the virtual crystal approximation.

calculations. Also the bands situated between 3 and 10 eV can be found in the calculated DOS. Our results show the qualitative agreement between calculations obtained with the correlation energy within the Fe and Ti 3d bands and partial DOS derived from the resonance photoemission for photon energy ascribed to Fe^{3+}. The used method of calculations does not assume any valence of doping ions, but we can notice that the iron contribution to the valence band is close to that of a trivalent ion. Our results are in agreement with Bader analysis showed in Table I. The presented results show similar values as for Fe_2O_3; hence, the presence of the Fe^{3+} is more probable. Most results from the literature are based on the presence of Fe^{4+} states for Fe substituting Ti.[9–11] However, da Silva *et al.* and Blokhin *et al.* found in Fe K edge x-ray absorption near-edge structure (XANES) an indication to the lower oxidation state.[9,12] Moreover, one has to remember that calculations were performed in the ground state and final state effects inseparably related to photoemission were not included.

It is worth noting that Fe is in the high spin state and the magnetic moment is 3.89 μ_B per Fe atom. It is in agreement with the observed quenching of the XAS Fe L_2 edge.

On the other hand, our results can be compared to the resonant photoemission data for Fe oxides published by Lad and Henrich.[28] They analyzed resonantly enhanced photoemission through the Fe 3p-3d excitation threshold for Fe_xO, Fe_2O_3, and Fe_3O_4, so for the compounds with primarily 2+, pure 3+, and mixed 3+ and 2+ Fe valence. Interestingly, the structure of the Fe 3d states for Fe_2O_3 has several features similar to our PDOS for Fe^{3+}, like the clear peak at about 3 eV, broad feature in the region 5–8 eV, and another one at 12–13 eV. It can be understood when taking into account the structure of Fe_2O_3 where the Fe^{3+} cation is surrounded by a distorted octahedron of O^{2-} ions. The mostly divalent Fe in Fe_xO shows the main features at 1.2 eV and 4.1 eV, and again this tendency is reflected in our Fe PDOS ascribed to Fe^{2+} states. Also for this compound, most Fe cations have the octahedral coordination.

For better understanding of the defect chemistry, relation between the Fe valence state and oxygen deficit, the samples were preheated in an ultra-high vacuum at 630 °C for 15 min. As it was suggested in the previous paper, such annealing leads to the increase of the oxygen vacancies in the surface region, and consequently to relative increase of the Fe^{2+} species which are connected to oxygen vacancies.[15] However, as can be seen in Fig. 4, the effect of the films annealing at 630 °C is very weak. A slight increase of the density of states in the gap is visible for the resonance related to Fe^{2+} ions for both samples doped with 2% and 5% Fe. The Fe^{3+} resonance shows a weak effect of annealing at higher temperatures visible as a slight decrease of the main peak at 2.5 eV. Such behavior can be understood as the effect of the additional oxygen vacancies formation in the surface region leading to the increase of the Fe^{2+}/Fe^{3+} ratio.

Fe doping is nominally connected to substitution of Ti ions in the TiO_6 octahedra. As it was discussed in our earlier paper, the detected valence state of iron is 2+ or 3+. The main question concerned the number of oxygen vacancies associated with the Fe ions centering the octahedra. Calculations by Alexandrov *et al.* for Fe^{4+} showed the partly covalent bonding between Fe and O atoms.[11] On the other hand, Blokhin *et al.* showed that oxygen vacancies (V_O) were located in the first coordination of Fe^{3+} ions in the cathodic region of the electrocolored Fe-doped STO.[12] In order to simulate the presence of oxygen vacancies in the perovskite lattice, we performed calculations within virtual crystal approximation, where an atom with a reduced atomic number was placed at all oxygen positions. Such a theoretical model shows at least a tendency for a very statistical and uniform distribution of vacancies. The results shown in Fig. 6(b) indicate the tendency to decrease the bandgap width and the shift of the structures within the PDOS's from Fe and Ti toward lower binding energies.

Thus, the calculations agree generally with the observation of the behavior ascribed to Fe^{2+}. One can state that the reduced valence of iron ions is related to the presence of vacancies, but further studies are necessary to find a clear relation between the observed structure of the valence band and number or distribution of vacancies. A possible explanation of the

TABLE I. The result of Bader charge analysis.

	Without U	With U
FeO	1.287	1.371
Fe_2O_3	1.44	1.546
$SrTiO_3$	1.56	1.556

discrepancies between experiment and calculations can be related to agglomeration of the Fe ions and oxygen vacancies forming extended defect complexes.[15]

Zhou *et al.* calculated DOS for Fe doped STO at two concentrations of 5% and 12.5% and Fe in the Ti and Sr sites.[10] They found a significant contribution of Fe originating states to the in-gap region. Despite the wrong value of the energy gap coming from the used method linear augmented plane wave (LAPW) with general gradient approximation (GGA) of exchange - correlation potential, the relatively broad band of Fe states spreading from the top of the valence band to about 1 eV below the bottom of the conduction band was obtained for Fe at the Ti site. For Fe at the Sr site, two sharp peaks of PDOS within the gap were found. Our results agree qualitatively with the case of 5% Fe at the Ti site.

To check the possible correlation between titanium and iron states, the photoemission studies of titanium electronic states were performed. For this reason, we measured the XAS spectra for all samples at the energy range assigned to the titanium $L_{2,3}$ absorption edge. An example of the spectrum for STO:2% Fe is presented in Fig. 7. For all investigated samples, the XAS spectrum had the same shape. It consists of four well separated peaks at 458.4 eV, 460.8 eV, 463.8 eV, and 466.1 eV. All spectra also showed two small pre-peaks at energies below 458.4 eV. The first of two main peaks, marked as "A" and "B" can be assigned to the L_3 edge (t_{2g} and e_g orbitals, respectively) and the second two ("C" and "D") to the L_2 edge (t_{2g} and e_g, respectively). The structure of the obtained XAS spectra is in accordance with the published data for STO.[29]

To calculate PDOS of titanium, the "B" peak (460.8 eV) was chosen to perform the "on resonance" measurements of the valence band electronic states. For the "off-resonance" measurements, the photon energy was chosen to be 452.8 eV. The selection of the resonance energy was caused by the presence of the feature coming from the second order light visible as a line crossing the binding energy region from −2 to 2 eV in the lower right corner of the photoemission map (Fig. 8). This feature comes from the known problem with the grating monochromators used for soft x-rays which produce higher order diffraction light, and the energy dependence of any photoemission structure having much higher binding energy leads

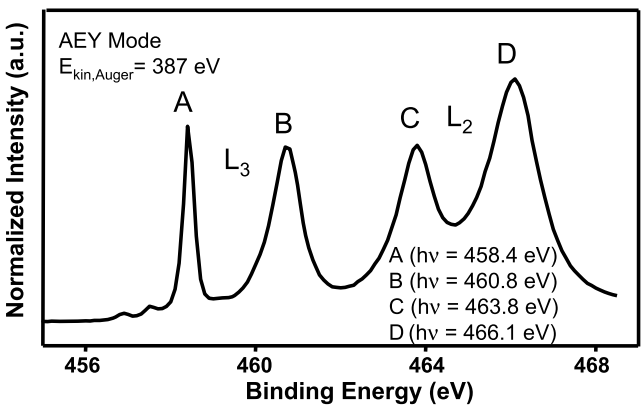

FIG. 7. Ti L edge x-ray absorption spectrum obtained in the Auger electron yield mode for the STO film doped with 2% Fe.

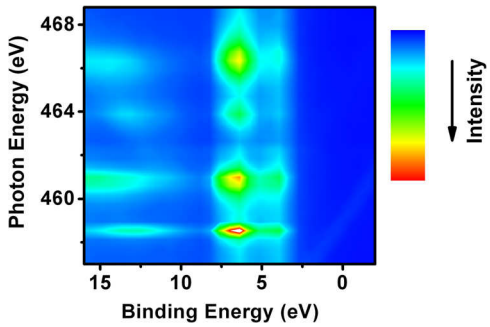

FIG. 8. Photoemission intensity maps in the valence band region obtained for the 1% Fe doped STO film for photon energies within the Ti 2p-3d resonance.

to the observed behavior of such a structure in the function of photon energy and binding energy. In our case, it disturbed the observation of very weak effect in the energy gap region. The photoemission map shows the valence band photoemission of the STO:1% Fe film for photon energy range of the $L_{2,3}$ Ti absorption edge. The films with higher Fe content showed an analogous behavior with slight differences observed within the energy gap region. Contrary to the photoemission map of the Fe resonance, there is no damping of the intensity from the L_2 edge, caused by a lack of spin polarization of Ti states.

The main contribution of titanium states to the valence band is visible in the range 3–8 eV. This behavior was observed also in the STO bulk crystals.[30,31] Additionally, we found the states originating from Ti in the energy region 10–16 eV. Due to the observed photon energy dependence, one can attribute them to the Auger transitions.[32] Analysis of the photoemission map does not indicate any significant contribution of Ti states to the energy gap region. To observe a possible weak intensity in that region, we calculated Ti PDOS in similar way as in the case of iron.

In Fig. 9, the in-gap PDOS for titanium is presented for selected films and two temperatures of annealing. The increasing intensity for energies above the Fermi level is due to the earlier mentioned second order light from the monochromator. The spectra were normalized to the intensity of the main

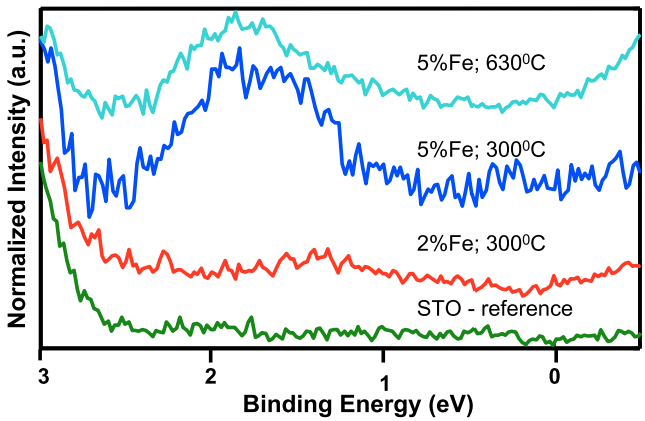

FIG. 9. The in-gap region of the valence band being a part of the Ti PDOS obtained by subtracting the photoemission spectra recorded at photon energies of 460.8 eV (on resonance) and 452.8 eV (off resonance). The spectra were normalized to the intensity at the main contribution to the valence band at 6.5 eV, not shown. Increasing intensity above the Fermi level comes from the second order light.

peak in the valence band situated at the energy of 6.5 eV. It is known that Ti^{3+} states give a contribution to the in-gap region in reduced or electron doped STO.[16,33] The appearance of the Ti^{3+} states can be related to the presence of oxygen vacancy and/or neighbouring electron donor. Ishida *et al.* distinguished the coherent states, which were situated at the Fermi level, and incoherent ones which were ascribed to the local Ti^{3+} states.[16] The contribution in the energy range 1–2 eV has been ascribed to Ti^{3+} incoherent states.[16] It is worth to mention that we found no reduced Ti states within the photoemission Ti 2p multiplets. However, the resonant photoemission clearly shows a Ti contribution to the in-gap states which is higher for the Fe doped films. Fe doping clearly increases this contribution although also for those films, we found no reduced Ti states within the Ti 2p photoemission. The reason is that the resonant photoemission is able to detect much lower concentrations of these states due to the strong enhancement of emission from the Ti 3d band.

Our calculations shown in Fig. 6(b) indicated the presence of Ti 3d states in the gap for Fe doped STO which is the result of hybridization with the Fe 3d states. A similar effect was found in calculations of Alexandrov *et al.*[11] and Zhou *et al.*[10] This effect can be responsible for the increasing Ti PDOS with Fe doping level observed in our studies. Introduction of oxygen vacancies in our calculations in the neighbourhood of Fe ions increases the density of Ti originating states in the bandgap region, especially at highest energies within the valence band. It is in agreement with the Fe PDOS obtained from the experiment.

Thus, one could attribute the observed intensity at energies of about 1.5–1.8 eV to the hybridization between Fe and Ti 3d states and to the formation of complexes Ti–V_O–Fe. As the intensity of the in-gap states is very low and the contribution from Ti in that energy range is much lower than that for Fe, one can relate the states visible in Ti PDOS to the agglomerated complexes in a form of extended defects or to the more complex distribution of oxygen vacancies. It is not clear why maximum of the Ti contribution to the in-gap states is shifting with Fe doping level.

Calculations taking into account various configurations of localized complexes with oxygen vacancies are necessary to obtain a more precise image of the electronic structure of Fe doped STO.

IV. CONCLUSIONS

The electronic structure of Fe doped epitaxial films of STO has been studied by the use of resonant photoemission and compared to *ab initio* calculations. Based on our earlier analysis of the XAS, the Fe contribution to the valence band was divided into two parts related to the Fe nominal valence states 2+ and 3+. These valence states result from different contributions to the valence band, especially within the in-gap region. The Fe^{3+} states form a sharp peak just above the top of the valence band, while Fe^{2+} contribute as a rather broad feature situated in the binding energy range below 0.5 eV. No states at the Fermi level were observed. Resonant photoemission at the Ti 2p-3d edge showed an in-gap contribution from the Ti states increasing with Fe doping level. The effect can be attributed to the hybridization between the Ti and Fe originating electronic states and to the presence of Ti states associated with Fe ions forming complexes with oxygen vacancies. The obtained partial DOS's are in qualitative agreement with the calculations performed by the FP-LAPW/APW+lo method for the 3.7% Fe doping level in STO including the correlation energy for the 3d levels of Fe and Ti. The presence of oxygen vacancies approached with the use of virtual crystal approximation affected the density of states within the band gap region in a way enabling their association to the nominal Fe^{2+} states. Further studies are necessary to clarify the relation between the nominal valence of doping ions and the electronic structure determined by experiment.

ACKNOWLEDGMENTS

This work was supported by the NCBiR as well as the NRW Bank within the Project No. ERA-NET-MATERA/3/2009. The work was also partially funded by the Deutsche Forschungsgemeinschaft SFB 917 ("Nanoswitches"). The assistance of Karina Shulte at the I311 beamline at Max-Lab is greatly appreciated.

[1] H. Y. Hwang, Y. Iwasa, M. Kawasaki, B. Keimer, N. Nagaosa, and Y. Tokura, "Emergent phenomena at oxide interfaces," Nat. Mater. **11**, 103–113 (2012).
[2] K. Szot, W. Speier, G. Bihlmayer, and R. Waser, "Switching the electrical resistance of individual dislocations in single-crystalline $SrTiO_3$," Nat. Mater. **5**, 312–320 (2006).
[3] F. J. Morin and J. R. Oliver, "Energy levels of iron and aluminum in $SrTiO_3$," Phys. Rev. B **8**, 5847–5854 (1973).
[4] R. Waser, T. Bieger, and J. Maier, "Determination of acceptor concentrations and energy levels in oxides using an optoelectrochemical technique," Solid State Commun. **76**, 1077–1081 (1990).
[5] R. Merkle and J. Maier, "How is oxygen incorporated into oxides? A comprehensive kinetic study of a simple solid-state reaction with $SrTiO_3$ as a model material," Angew. Chem., Int. Ed. **47**, 3874–3894 (2008).
[6] R. Moos and K. H. Hardtl, "Defect chemistry of donor-doped and undoped strontium titanate ceramics between 1000° and 1400 °C," J. Am. Ceram. Soc. **80**, 2549–2562 (2005).
[7] T. Takeda, Y. Yamaguchi, and H. Watanabe, "Magnetic structure of $SrFeO_3$," J. Phys. Soc. Jpn. **33**, 967–969 (1972).
[8] L. F. da Silva, M. I. B. Bernardi, L. J. Q. Maia, G. J. M. Frigo, and V. R. Mastelaro, "Synthesis and thermal decomposition of $SrTi_{1-x}Fe_xO_3$ ($0.0 \leq x \leq 0.1$) powders obtained by the polymeric precursor method," J. Therm. Anal. Calorim. **97**, 173–177 (2009).
[9] L. F. da Silva, J.-C. M'Peko, J. Andrés, A. Beltrán, L. Gracia, M. I. B. Bernardi, A. Mesquita, E. Antonelli, M. L. Moreira, and V. R. Mastelaro, "Insight into the effects of Fe addition on the local structure and electronic properties of $SrTiO_3$," J. Phys. Chem. C **118**, 4930–4940 (2014).
[10] X. Zhou, J. Shi, and C. Li, "Effect of metal doping on electronic structure and visible light absorption of $SrTiO_3$ and $NaTaO_3$ (metal = Mn, Fe, and Co)," J. Phys. Chem. C **115**, 8305–8311 (2011).
[11] V. Alexandrov, J. Maier, and R. A. Evarestov, "*Ab initio* study of $SrFe_xTi_{1-x}O_3$: Jahn-Teller distortion and electronic structure," Phys. Rev. B **77**, 075111 (2008).
[12] E. Blokhin, E. Kotomin, A. Kuzmin, J. Purans, R. Evarestov, and J. Maier, "Theoretical modeling of the complexes of iron impurities and oxygen vacancies in $SrTiO_3$," Appl. Phys. Lett. **102**, 112913 (2013).
[13] Ch. Lenser, A. Kuzmin, J. Purans, A. Kalinko, R. Waser, and R. Dittmann, "Probing the oxygen vacancy distribution in resistive switching Fe-$SrTiO_3$ metal-insulator-metal-structures by micro-x ray absorption near-edge structure," J. Appl. Phys. **111**, 076101 (2012).
[14] J. Szade, K. Szot, M. Kulpa, J. Kubacki, Ch. Lenser, R. Dittmann, and R. Waser, "Electronic structure of epitaxial Fe-doped $SrTiO_3$ thin films," Phase Transitions **84**, 489–500 (2011).
[15] A. Koehl, D. Kajewski, J. Kubacki, Ch. Lenser, R. Dittmann, P. Meuffels, K. Szot, R. Waser, and J. Szade, "Detection of Fe^{2+} valence states in Fe doped $SrTiO_3$ epitaxial thin films grown by pulsed laser deposition," Phys. Chem. Chem. Phys. **15**, 8311–8317 (2013).

[16]Y. Ishida, R. Eguchi, M. Matsunami, K. Horiba, M. Taguchi, A. Chainani, Y. Senba, H. Ohashi, H. Ohta, and S. Shin, "Coherent and incoherent excitations of electron-doped $SrTiO_3$," Phys. Rev. Lett. **100**, 056401 (2008).
[17]A. F. Santander-Syro, O. Copie, T. Kondo, F. Fortuna, S. Pailhès, R. Weht, X. G. Qiu, F. Bertran, A. Nicolaou, A. Taleb-Ibrahimi, P. Le Fèvre, G. Herranz, M. Bibes, N. Reyren, Y. Apertet, P. Lecoeur, A. Barthélémy, and M. J. Rozenberg, "Two-dimensional electron gas with universal subbands at the surface of $SrTiO_3$," Nature **469**, 189–193 (2011).
[18]Y. J. Chang, A. Bostwick, Y. S. Kim, K. Horn, and E. Rotenberg, "Structure and correlation effects in semiconducting $SrTiO_3$," Phys. Rev. B **81**, 235109 (2010).
[19]P. Blaha, K. Schwarz, G. K. H. Madsen, D. Kvasnicka, and J. Luitz, *WIEN2k, An Augmented Plane Wave + Local Orbitals Program for Calculating Crystal Properties*, Karlheinz Schwarz (Technische Universität Wien, Austria, 2001), ISBN: 3-9501031-1-2.
[20]J. P. Perdew and Y. Wang, "Accurate and simple analytic representation of the electron-gas correlation energy," Phys. Rev. B **45**, 13244 (1992).
[21]D. M. Ceperley and B. J. Alder, "Ground state of the electron gas by a stochastic method," Phys. Rev. Lett. **45**, 566 (1980).
[22]V. I. Anisimov, I. V. Solovyev, M. A. Korotin, M. T. Czyżyk, and G. A. Sawatzky, "Density-functional theory and NiO photoemission spectra," Phys. Rev. B **48**, 16929 (1993).
[23]F. M. F. de Groot, P. Glatzel, U. Bergmann, P. A. van Aken, R. A. Barrea, S. Klemme, M. Hävecker, A. Knop-Gericke, W. M. Heijboer, and B. M. Weckhuysen, "1s2p resonant inelastic x-ray scattering of iron oxides," J. Phys. Chem. B **109**, 20751–20762 (2005).
[24]W. M. Heijboer, A. A. Battiston, A. Knop-Gericke, M. Hävecker, H. Bluhm, B. M. Weckhuysen, D. C. Koningsberger, and F. M. F. de Groot, "Redox behaviour of over-exchanged Fe/ZSM5 zeolites studied with *in-situ* soft x-ray absorption spectroscopy," Phys. Chem. Chem. Phys. **5**, 4484–4491 (2003).
[25]Y. Adachi, S. Kohiki, K. Wagatsuma, and M. Oku, "Intrinsic and extrinsic surface states of single crystalline $SrTiO_3$," J. Appl. Phys. **84**, 2123 (1998).
[26]I. Denk, W. Münch, and J. Maier, "Partial conductivities in $SrTiO_3$: Bulk polarization experiments, oxygen concentration cell measurements, and defect-chemical modeling," J. Am. Ceram. Soc. **78**, 3265–3272 (1995).
[27]A. Rothschild, W. Menesklou, H. L. Tuller, and E. Ivers-Tiffée, "Electronic structure, defect chemistry, and transport properties of $SrTi_{1-x}Fe_xO_{3-y}$ solid solutions," Chem. Mater. **18**, 3651–3659 (2006).
[28]R. J. Lad and V. E. Henrich, "Photoemission study of the valence-band electronic structure in Fe_xO, Fe_3O_4, and α-Fe_2O_3 single crystals," Phys. Rev. B **39**, 13478 (1988).
[29]F. M. F. de Groot, "X-ray absorption and dichroism of transition metals and their compounds," J. Electron Spectrosc. Relat. Phenom. **67**, 529–622 (1994).
[30]Y. Haruyama, S. Kodaira, Y. Aiura, H. Bando, Y. Nishihara, T. Maruyama, Y. Sakisaka, and H. Kato, "Angle-resolved photoemission study of $SrTiO_3$ (100) and (110) surfaces," Phys. Rev. B **53**, 8032 (1996).
[31]M. Takizawa, K. Maekawa, H. Wadati, T. Yoshida, A. Fujimori, H. Kumigashira, and M. Oshima, "Angle-resolved photoemission study of Nb-doped $SrTiO_3$," Phys. Rev. B **79**, 113103 (2009).
[32]T. Kaurila, R. Uhrberg, and J. Väyrynen, "2p-3d resonant photoemission in Ti metal," J. Electron Spectrosc. Relat. Phenom. **88**, 399–403 (1998).
[33]Y. Aiura, I. Hase, H. Bando, T. Yasue, T. Saitoh, and D. S. Dessau, "Photoemission study of the metallic state of lightly electron-doped $SrTiO_3$," Surf. Sci. **515**, 61–74 (2002).